Results in Surfaces and Interfaces 22 (2026) 100727

Contents lists available at ScienceDirect

Results in Surfaces and Interfaces

journal homepage: www.elsevier.com/locate/rsurfi

Surface functionalization of medical-grade polyvinyl chloride treated with ammonia plasma

Rok Zaplotnik [a,*], Nina Recek [a], Gregor Primc [a], Andrej Gyergyek [b], Marian Lehocky [c], Miran Mozetič [a], Alenka Vesel [a]

[a] Jozef Stefan Institute, Department of Surface Engineering, Jamova cesta 39, 1000, Ljubljana, Slovenia
[b] Division of Surgery, University Medical Centre, Zaloška cesta 7, 1000, Ljubljana, Slovenia
[c] Centre of Polymer Systems, Tomas Bata University in Zlín, Třída Tomáše Bati 5678, 760 01, Zlín, Czech Republic

ARTICLE INFO

Keywords:
PVC polymer
Ammonia plasma
Surface modification
Chlorine
Medical application

ABSTRACT

Polyvinyl chloride (PVC) is often the material of choice for the synthesis of various components used in medical practice, particularly catheters. As-synthesized components may not exhibit appropriate biocompatibility, so the surface should be modified or coated. Amine groups were grafted onto the PVC surface by brief exposure to ammonia plasma generated by a low-pressure inductively coupled radiofrequency discharge in E mode (30 Pa, 25 W). The treatment time ranged from 0.5 to 300 s. The measured density of charged particles was approximately $2 \pm 1 \times 10^{15}$ m^{-3} and the flux of NH and NH_2 radicals was approximately 3×10^{23} $m^{-2}s^{-1}$. X-ray photoelectron spectroscopy (XPS) was used to study the evolution of nitrogen-containing functional groups versus the treatment time. The chlorine concentration was not affected much, but the nitrogen concentration in the surface film increased logarithmically with increasing treatment time. The N concentration was approximately 2 at.% after 0.5 s of treatment and reached approximately 9 at.% after 300 s. Some PVC samples were also pretreated with hydrogen plasma. The pretreatment was beneficial for rapid functionalization, as the N concentration reached 6 at.% after 0.5 s of plasma treatment, but the concentration after prolonged treatment was the same as that for a single-step ammonia plasma treatment. High-resolution XPS Cl2p spectra revealed significant modification of the chlorine binding, especially after pretreatment with hydrogen plasma. A possible explanation for this modification is the formation of Cl^- binding states, resulting from bond scission by the absorption of VUV radiation in the PVC surface film.

1. Introduction

The surface properties of polymers are rarely adequate for many applications, so they should be modified. A standard method for the surface modification of many polymers is the application of non-equilibrium gaseous plasma [1]. Depending on the gas type and discharge conditions, a variety of surface functional groups can be generated upon plasma treatment [2–7]. Of particular interest is the formation of amine groups on the surface of polymers for biomedical applications. Recent advances in biomedical coatings include the application of anticoagulation and anti-fouling properties, as shown by several teams worldwide [8–13]. The amine groups are usually grafted onto a polymer surface by treating the samples with plasma sustained in ammonia. Functionalization with amine groups often improves the biocompatibility of polymer implants by enabling covalent or electrostatic bonding of a thin heparin layer to otherwise fairly inert polymers [14]. The basic mechanism of interaction of blood constituents with the heparin molecules has been known for decades [15]. Briefly, heparin is among the best-known anticoagulants [16]. It interacts with antithrombin, which causes a different conformation of this blood protein. As a result, the complex inhibits factors that are responsible for blood clotting, particularly thrombin. That is why surface functionalization of standard polymers used for synthesizing body implants with amino groups has attracted significant attention from the scientific community.

The ammonia molecule will decompose under plasma conditions [17–19]. High power density plasmas enable extensive decomposition [20,21], which may not be practical for the grafting of the polymer surfaces with -NH_2 groups. Opposite, plasma sustained in a mixture of nitrogen and hydrogen was also found interesting for the synthesis of

* Corresponding author.
E-mail address: rok.zaplotnik@ijs.si (R. Zaplotnik).

https://doi.org/10.1016/j.rsurfi.2026.100727
Received 2 July 2025; Received in revised form 22 January 2026; Accepted 26 January 2026
Available online 28 January 2026

ammonia [22]. There is a balance between the decomposition of NH_3 and synthesis, but the details are yet to be elaborated. Weakly ionized ammonia plasma will favor partial dissociation of NH_3 molecules to form NH_2 and some NH radicals, while powerful plasma will cause extensive dissociation, and the resultant N and H atoms are likely to form N_2 and H_2 molecules by heterogeneous surface recombination [23]. NH_x radicals (x = 1 or 2) are suitable for the surface functionalization of hydrocarbons like polymers [24], but they also cause significant etching, leading to the formation of HCN [25]. Ammonia plasma has been used for the surface functionalization of different polymers, and a brief review is provided below.

Young et al. [26] treated polyether ether ketone with ammonia plasma, and various peptides were conjugated to plasma-treated samples. They observed improved endothelialization and anti-thrombogenic properties. The plasma treatment times were 1, 10, and 20 min, but other details about the treatment parameters were not disclosed. The concentration of nitrogen in the surface film of the thickness as probed by XPS was up to 14 at.%.

Islam et al. [27] treated polystyrene films with plasma sustained in a mixture of argon and ammonia with the flow rates of 10 and 25 sccm. Plasma was sustained by a capacitively coupled RF discharge at a power of 20 W, and the treatment time was 5 min. XPS survey spectra showed 7 at.% nitrogen, but as much as 35 at.% of oxygen, so the polystyrene surface was probably also functionalized with amide groups, apart from oxygen functional groups.

Buddhadasa et al. [28] treated activated carbon monoliths with ammonia plasma sustained at a pressure of 80 Pa by an electrodeless capacitively coupled RF discharge. The discharge power was varied from 2 to 15 W, the gas flow rate was 20 sccm, and the treatment time was 5 min. The authors reported N concentrations ranging from 4 to 14 at.%, and the results were highly scattered, so no correlation between the processing parameters and the N concentration on the polymer surface could be inferred.

Peixoto et al. [29] treated polyethylene terephthalate and polylactic acid yarns with ammonia plasma and obtained functionalization with amine groups without measurable modification of the morphology or mechanical properties. Plasma was sustained by an asymmetric capacitively coupled RF discharge operating at a pressure of 7 or 11 Pa. The treatment time varied between 3 and 20 min. A colorimetric assay with Orange II was used to quantitatively evaluate the concentration of amine groups on the polymer surfaces. The results were scattered, but all treatment times resulted in a several-fold increase in the absorbance. The 12-min treatment at 7 Pa was found to be the best, as the absorbance increased 6- and 10-times for polyethylene terephthalate and polylactic acid, respectively. The surface modification was stable for at least one month.

Mora-Cortes et al. [30] treated polyethylene terephthalate in plasma sustained in a mixture of diethylenetriamine or ethylenediamine and residual atmosphere in a simple vacuum system. The ultimate pressure was 15 Pa. The discharge powers were 150, 175, and 200 W, and the treatment time was 5, 10, or 15 min. Plasma treatment under these conditions caused a moderately hydrophilic surface finish with a water contact angle of 30–50°. The results were scattered, so no correlation between the wettability and treatment time or discharge power was obvious. Interestingly, XPS revealed the O concentration as low as 5 at.% on the surface of pristine PET. The oxygen concentration increased to about 10 at.% after 15 min at 200 W, and the concentration of nitrogen was as large as about 20 at.%. Several pathways were proposed, but all took into account both oxidation because of the large partial pressure of the residual atmosphere and grafting of amine-rich substances by plasma polymerization.

Formation of the amine and oxygenated functional groups on the nanocarbon surface upon treatment with ammonia plasma was also reported by Benlikaya et al. [31]. The pressure was adjusted to 40 or 300 Pa, and the treatment time was 10 min. Plasma was sustained by an inductively coupled RF discharge, and the maximal power of the RF generator was 1500 W. XPS showed rich surface functionalization. The formation of oxygen-rich functional groups was attributed to the residual atmosphere. A variety of possible reactions on the carbon surface with various species in ammonia plasma were proposed. The plasma pretreatment was used to synthesize epoxy-nanocarbon composites.

The surface functionalization of a fluorinated polymer upon treatment with ammonia plasma was reported by Vesel et al. [32]. Unlike previously cited authors, Vesel et al. adopted a two-step plasma treatment. In the first step, they treated polytetrafluoroethylene with hydrogen plasma for 1 s, and then they exposed such pretreated samples to ammonia plasma. Ammonia pressure was 35 Pa, and the discharge power was 200 W. The nitrogen concentration on the polymer surface was about 10 at.%. Angular-resolved high-resolution XPS confirmed the substitution of C-F surface bonds with nitrogen-containing groups.

The brief literature survey reveals that different teams used various discharges to sustain ammonia plasma and treat polymer materials. The typical treatment time was of the order of a minute. No author reported plasma parameters, so it is not feasible to draw general conclusions.

We focused our study on medical-grade poly(vinyl chloride), which is often used for synthesizing medical products like catheters [33–37]. Medical-grade PVC contains about 60 % PVC resin; the remaining 40 % are additives, especially plasticizers, which provide appropriate mechanical properties and stability and prevent the release of HCl during hot deformation [38]. The exact composition of such materials is usually not disclosed and probably varies between the producers. The plasticizers are organic molecules that contain a significant concentration of oxygen [39]. Organometallic compounds containing tin are also added to improve the properties of PVC products [40,41]. The PVC may not be the optimal material for the manufacture of medical devices, because of the leaching of plasticizers, which may reduce biocompatibility and lead to possible complications associated with the estrogenic-like properties of some additives [42]. Possible toxicity was considered by an EU working group, but it could not provide specific recommendations to limit the use of PVC medical devices containing plasticizers [43]. A recent EU report stressed possible negative effects of PVC on the environment [44]. A recent critical review on the environmental concerns was prepared by Kudzin et al. [45].

2. Experimental

2.1. Materials

Polyvinyl chloride (PVC) was supplied by Goodfellow Ltd (Huntington, UK). The thickness of the PVC foil was 0.2 mm. Square samples of 1 × 1 cm were cut from the foil for further experiments. After cutting a square sample, it was grasped with tweezers and mounted into the discharge tube without any other treatment, such as chemical cleaning.

2.2. Plasma reactor

Samples were treated in a plasma reactor illustrated in Fig. 1. The discharge tube with a diameter of 4 cm and a length of 80 cm is made from borosilicate glass, which is connected to standard vacuum flanges using rubber O-rings. The reactor is pumped on one side with a two-stage rotary pump with a nominal pumping speed of 80 m^3/h and an ultimate pressure of about 0.1 Pa. Pressure was measured with a capacitive gauge (Baratron 722A, MKS Instruments, Andover, USA) calibrated for the range between 1 and 1000 Pa. The pressure gained upon pumping for a few minutes was below the detection limit of the gauge (1 Pa). Ammonia was introduced into the discharge tube on the other side through a needle valve. The pressure at the vacuum gauge position was set to 30 Pa.

Plasma was sustained in the discharge tube with an RF generator (CESAR 1310, Advanced Energy Ltd, Denver, USA) operating at adjustable forward power up to 1000 W. The generator was coupled to a coil via a matching network. The forward power of 50 W was selected for

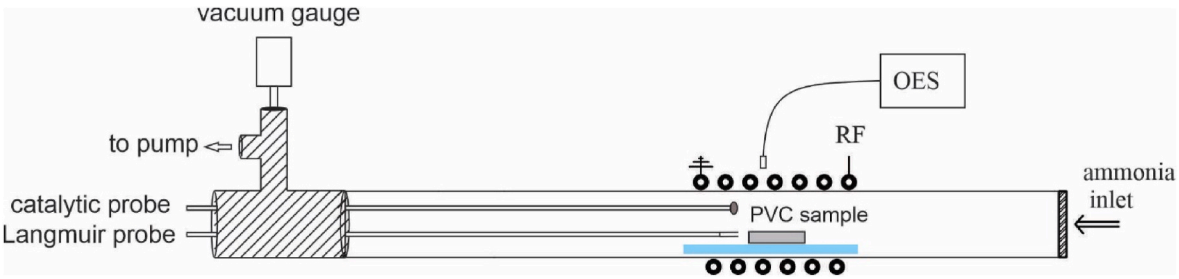

Fig. 1. Experimental setup.

our experiments. The reflected power was about 25 W, so the real power used for sustaining plasma was about 25 W.

Plasma was characterized by movable electrical and catalytic probes as well as optical emission spectroscopy. The electrical (Langmuir) probes were supplied by Impedans Ltd. (Dublin, Ireland), and the catalytic probe by Plasmadis d. o.o. (Ljubljana, Slovenia). Both tungsten single and tungsten double Langmuir probes were used to measure plasma density. A single probe tip was a metal rod with a diameter of 0.39 mm, where 10 mm of the probe's tip length was exposed to plasma. A double probe was made from two tungsten rods with the same exposed length and diameter, which were 2.5 mm apart. The catalytic probe had a cobalt disk tip with a thickness of 0.05 mm and a diameter of 3 mm. Optical emission spectroscopy (OES) of plasma was performed using an AvaSpec-3648 Fiber Optic Spectrometer (Avantes, Apeldoorn, Netherlands). The resolution of the spectrometer was 0.5 nm. The integration time was 10 s when measuring the spectrum and 2 s when measuring the time evolution of selected spectral lines.

2.3. Plasma treatment of polymer samples

PVC samples were placed inside the copper coil in the system shown in Fig. 1. Two different treatments in ammonia plasma were performed, i.e., without or with pretreatment in hydrogen plasma. In the first case (without pretreatment), the system was evacuated to a pressure below the detection limit of the gauge, and the ammonia was leaked into the discharge tube. The RF generator was turned on to enable surface modification of the PVC samples for selected treatment times ranging from 0.5 to 300 s. When the plasma treatment was accomplished, the RF generator was turned off, the system was vented, and the sample was installed in the XPS instrument. Several treatment times were selected, and each treatment was performed using a fresh PVC sample. Within an hour of the plasma treatment, the samples were probed by XPS, and both survey and high-resolution spectra were acquired.

In the second case, PVC samples were modified using an additional pretreatment step in hydrogen plasma. Hydrogen was introduced after evacuation of the discharge tube, and plasma was ignited just for 1 s. The discharge power for sustaining hydrogen plasma was set to 400 W, and the hydrogen pressure was 22 Pa. After treating the samples with hydrogen plasma, the reactor was evacuated again without venting or breaking the vacuum conditions. Instead, ammonia was introduced in the reactor, so the PVC samples, which had been pretreated with hydrogen plasma, were exposed to ammonia plasma.

2.4. Surface characterization

PVC samples were characterized by X-ray photoelectron spectroscopy (XPS). A spectrometer TFA XPS (Physical Electronics, Munich, Germany) was used. The samples were exposed to monochromatic Al $K\alpha_{1,2}$ radiation at a photon energy of 1486.6 eV. The spectra were recorded at an electron take-off angle of 45°. The survey spectra were acquired at a pass energy of 187 eV using an energy step of 0.4 eV. High-resolution C1s spectra were measured at a pass energy of 29.35 eV using an energy step of 0.125 eV. An additional electron gun was used to compensate for surface charge accumulation. The C1s peak corresponding to C–C bonds was set at 285 eV.

The measured spectra were analyzed using the MultiPak v8.1c software provided with the spectrometer. Shirley-type background subtraction was used. The spectra were fitted with Gauss-Lorentz functions. Detailed fitting was performed only for chlorine, where important changes were observed. Because chlorine is a doublet, it was fitted with two components ($2p_{3/2}$ in $2p_{1/2}$) separated by 1.6 eV. The area of the $2p_{1/2}$ component was fixed to 50 % of the value of the $2p_{3/2}$ component. The width of the peaks (FWHM) was fixed to 1.3 ± 0.1 eV.

The morphology of the PVC samples before and after plasma treatments was evaluated by atomic force microscopy. We used Solver PRO (NT-MDT) Atomic force microscope in contact mode in air. A standard Si cantilever with Au reflective side was used. The cantilever's tip radius was 10 nm, the tip length was 95 μm, and the scan rate was set at 1 Hz. Every measurement was repeated at least five times. Average surface roughness was determined with Gwyddion software.

3. Results and discussion

3.1. Plasma characterization

3.1.1. Optical emission spectroscopy

Plasma was characterized before treating polymer samples. Fig. 2 (a) shows a typical optical spectrum. Both atomic lines and molecular bands are revealed. The atomic lines include the Balmer series (transition from higher excited states to the first excited state of neutral hydrogen atoms). The high intensity of these lines is typical for plasmas sustained in gases containing hydrogen, like pure hydrogen or hydrocarbons. The intensive H peaks indicate qualitatively an adequate dissociation of ammonia molecules, i.e., the formation of H atoms and NH_x radicals. There is a continuum between roughly 450 and 800 nm. The continuum arises from radiative transitions of the NH_2 radicals. A higher-resolution spectrometer would reveal a rich vibrational population of the radiative states and the broadening of the vibrational transitions due to rotational excitation. As mentioned in the Experimental section, the spectrometer used for our experiments has a moderate resolution, so it is not possible to detect the fine structure of NH_2 transitions. The height of this continuum is relatively low, but the integral intensity is much stronger than the intensity of the H lines. The H lines are very narrow. The large integral intensity of this continuum indicates an adequate dissociation of ammonia molecules and a large density of NH_2 radicals.

An intense line is observed at the wavelength of approximately 336 nm. This line corresponds to the transition from the first electronic state and ground vibrational state of the NH radical to the ground electronic state (transition $A\ ^3\pi - X\ ^3\Sigma^-$). The large intensity indicates the formation of NH radicals, which is logical even though the discharge power density was relatively low in our experiments. More interesting is the appearance of the nitrogen molecular band in the ultraviolet range (transition $C\ ^3\pi_u - B\ ^3\pi_g$). Nitrogen was not leaked into the experimental system, and the system was hermetically sealed, so the source of N2 must be complete dissociation of ammonia, i.e., the formation of N atoms. The nitrogen molecules cannot be formed from N atoms in the gas

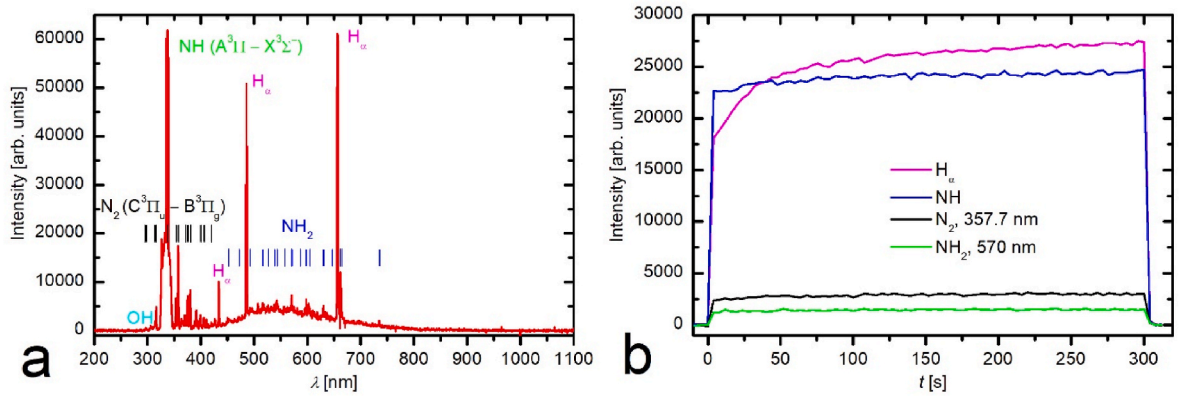

Fig. 2. A typical optical spectrum (a) and the time evolution of selected spectral lines (b).

phase at low pressure (because it requires a three-body collision to ensure conservation of energy and momentum), but are likely to appear because of the heterogeneous surface recombination of N atoms. The appearance of the N_2 band indicates that a fraction of the ammonia molecules is fully dissociated, even though the discharge power is moderate.

The above-mentioned transitions are marked in Fig. 2 (a). The H atoms also recombine on surfaces and form H_2 molecules. The radiative transitions from H_2 molecules should appear as the Fulcher band (roughly between 550 and 650 nm), but it overlaps with the NH_2 continuum.

Fig. 2 (b) shows the temporal evolution of selected spectral features. The curves are rather constant, so one can conclude that the plasma is rather stable. In fact, there are not many reasons for drifting plasma parameters with time because we kept the discharge parameters constant.

3.1.2. *Single and double electrical probe*

Optical emission spectroscopy is a qualitative technique for plasma characterization, so it does not reveal the density of radicals, let alone charged particles. The density of charged particles was determined with single and double Langmuir probes. The probe tips were positioned in the center of the coil (Fig. 1). Fig. 3 shows the typical current-voltage characteristics of both probes. Fig. 3 (a) is the I(U) characteristic of the single probe. The probe was biased with a variable DC power supply, and the tungsten rod served as the reference electrode. The ion-saturated current (below the voltage of about −5 V) is rather constant at −0.1 mA. The corresponding ion density in our plasma, as determined from the ion saturated current measured with the single probe, was 1×10^{15} m^{-3}. The electron density was also deduced from the characteristics shown in Fig. 3 (a). At the voltage of 30 V (at the inflection point on the curve), the electron current was approximately 2.5 mA. Based on the recommended interpretation, an electron density of approximately 3×10^{15} m^{-3} was determined.

The I(U) characteristics of a double probe is shown in Fig. 3 (b). The red curve presents the as-measured characteristics, and the black curve presents the characteristics corrected by the probe software. The characteristics is somewhat asymmetrical, but the ion-saturated current of the corrected curve is rather constant. The saturated current in Fig. 3 (b) was used to calculate the density of positive ions in the vicinity of the electrodes. The value was approximately 3×10^{15} m^{-3}. Double probes are not capable of measuring the electron density because only the electrons from the high-energy tail of the electron distribution function are capable of reaching the electrodes. The ion and electron densities should be the same because ammonia is not an electronegative gas. The differences in the plasma density as calculated from the characteristics of both probes are therefore attributed to the error arising from details whose explanations are beyond the scope of this article. The plasma density (i.e., density of charged particles) is rather low (a few 10^{15} m^{-3}), which is explained by a relatively low power (25 W) used for sustaining plasma.

3.1.3. *Catalytic probe*

Optical emission spectroscopy shows that any radiation arising from charged particles is marginal as compared to radiation from ammonia radicals (NH, NH_2, H), so the radical density should be much larger than the density of charged particles. The radical flux was determined from the characteristics of a catalytic probe, which is shown in Fig. 4 (a). Plasma was ignited for 20 s. Fig. 2 shows extensive heating of the catalytic probe due to the exothermic surface reactions on the catalytic tip. The predominant exothermic reaction in weakly ionized low-pressure plasmas sustained in molecular gases is surface recombination. OES

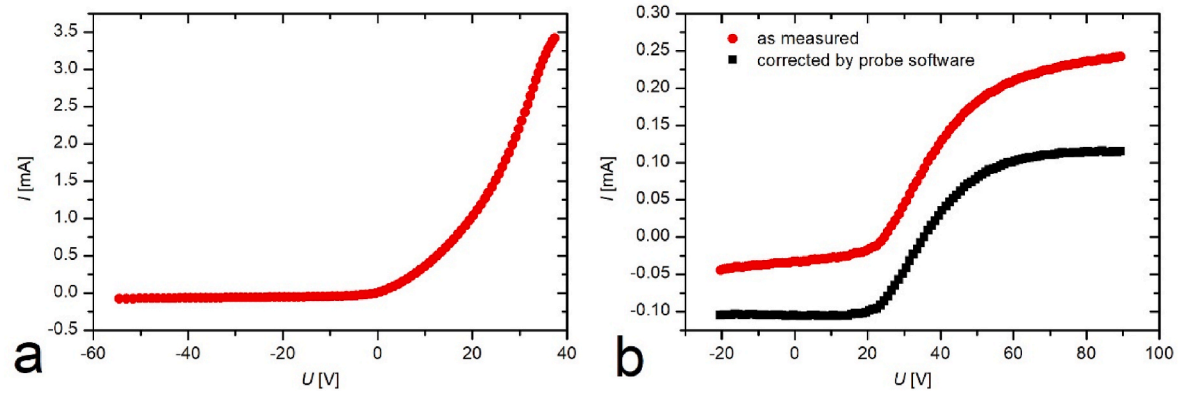

Fig. 3. Typical characteristics of a single (a) and a double (b) electrical probe.

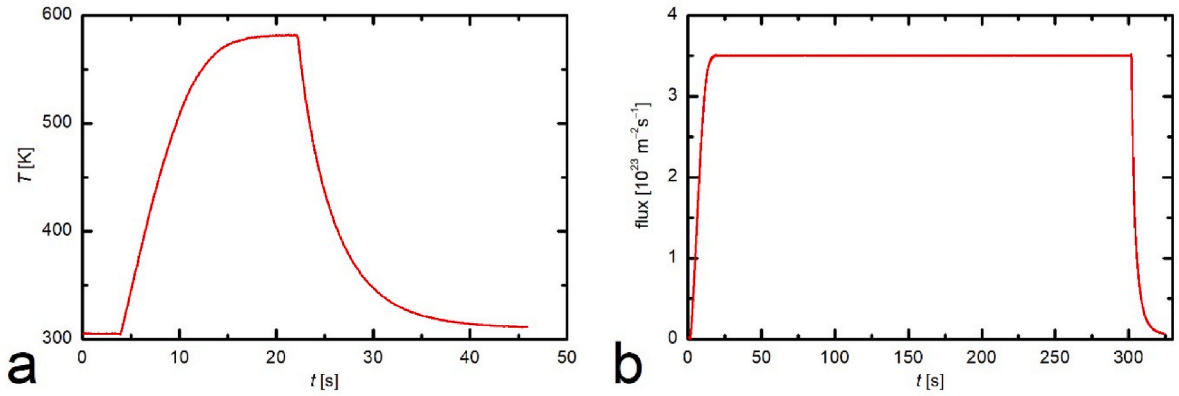

Fig. 4. (a) A typical signal of a catalytic probe, i.e., the temporal evolution of the probe tip temperature, and (b) the flux of radicals versus the plasma on time.

(Fig. 2 (a)) shows that both NH and NH_2 radicals are present, and the radiation from N_2 indicates that some N atoms are also present in the ammonia plasma. The flux of radicals is therefore a sum of H (predominant), NH_2, NH, and N. The flux is approximately 3×10^{23} $m^{-2}s^{-1}$. Taking into account the random movement of the plasma radicals, their density is estimated to be approximately 5×10^{20} m^{-3}. This value is a rough estimate due to the lack of reliable data on the heterogeneous surface reactions typical of weakly ionized ammonia plasma, but it is useful to conclude that the flux of neutral radicals is orders of magnitude larger than that of positively charged ions. The flux of radicals does not depend on the treatment time, as demonstrated in Fig. 4 (b). The response time of the catalytic probe is several s, so the increasing flux after turning on the discharge and decreasing after turning off are probe artefacts.

3.2. Surface characterization

3.2.1. Evolution of surface functional groups upon one-step ammonia plasma treatment

Fresh PVC samples were treated in the ammonia plasma. The survey spectra for all treated samples are shown in Fig. 5. The composition of the surface film of thickness probed by XPS is presented in Table 1. XPS cannot determine the hydrogen concentration. The pristine PVC (lowest curve in Fig. 5) contains carbon and chlorine, but the ratio is much lower

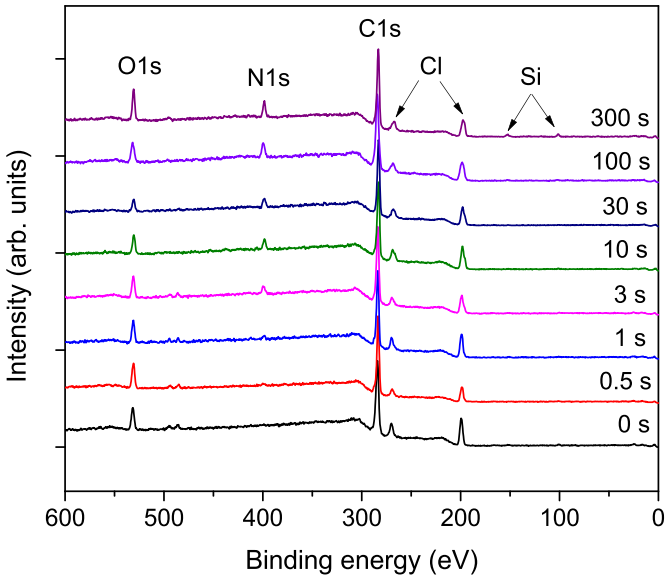

Fig. 5. The survey spectra of PVC samples treated in ammonia plasma. The treatment time is the parameter.

Table 1
The composition of the surface film for samples treated in ammonia plasma.

Time (s)	C (at. %)	N (at. %)	O (at. %)	Si (at. %)	Cl (at. %)	O/C	N/C	Cl/C
0.0	78.4	0.0	10.2	1.0	10.4	0.13	0.00	0.13
0.5	77.5	2.3	11.0	0.5	8.7	0.14	0.03	0.11
1	76.5	2.4	9.7	0.5	10.9	0.13	0.03	0.14
3	75.8	5.0	9.7	0.6	9.0	0.13	0.07	0.12
10	73.6	6.6	8.8	0.8	10.2	0.12	0.09	0.14
30	77.7	6.7	5.9		9.8	0.08	0.09	0.13
100	75.3	8.2	8.9	0.4	7.2	0.12	0.11	0.10
300	70.4	9.1	11.3	1.8	7.5	0.16	0.13	0.11

than the theoretical 2/3 carbon and 1/3 chlorine. The discrepancy is explained by the composition of the PVC samples. As mentioned in the Introduction, the pure PVC resin is unstable at elevated temperatures upon synthesizing the products and should be stabilized using various stabilizers, which contain carbon but not chlorine [38]. The stabilizers contain a significant concentration of oxygen [39–41], which explains the presence of approximately 10 at.% of oxygen (Fig. 5 and Table 1). XPS reveals minute concentrations of some other elements like Si and Sn. These also come from the stabilizers used in manufacturing PVS. The concentration of these elements is, however, marginal.

Treatment in ammonia plasma causes modifications in the surface composition. The only difference that is obvious when examining Fig. 1 is the appearance of nitrogen, whose peak increases with increasing treatment time. The N/C ratio (Table 1) increases monotonously with treatment time and reaches approximately 9 at.%, indicating significant functionalization with nitrogen-containing functional groups. There is little correlation between treatment time and the concentration of other elements. Still, the highest N concentrations are observed at the lowest Cl concentration, suggesting that some C-Cl bonds are replaced by N-containing functional groups.

High-resolution XPS spectra (HR-XPS) reveal the chemical environment of selected atoms in the surface film. The spectra for carbon, chlorine, oxygen, and nitrogen are plotted in Fig. 6. The shape of the high-resolution spectra changes significantly for samples exposed to plasma for different treatment times, which indicates an important modification of the surface chemistry. Let us first examine the evolution of C1s spectra, which are shown in Fig. 6 (a). There are some slight differences in the shape of these spectra, but they are not conclusive. The reason is the overlapping of peaks attributed to various functional groups. For example, the C-N bond should appear at 285.4–286.4 eV, and this binding energy overlaps with C-O (286–286.7 eV), and C-C-Cl/C-Cl (286–287 eV) [46].

The surface modifications are more evident from HR-XPS Cl2p spectra, which are shown in Fig. 6 (b). One can observe a doublet with peaks at 200 eV ($2p_{3/2}$) and 201.7 eV ($2p_{1/2}$) for an untreated sample.

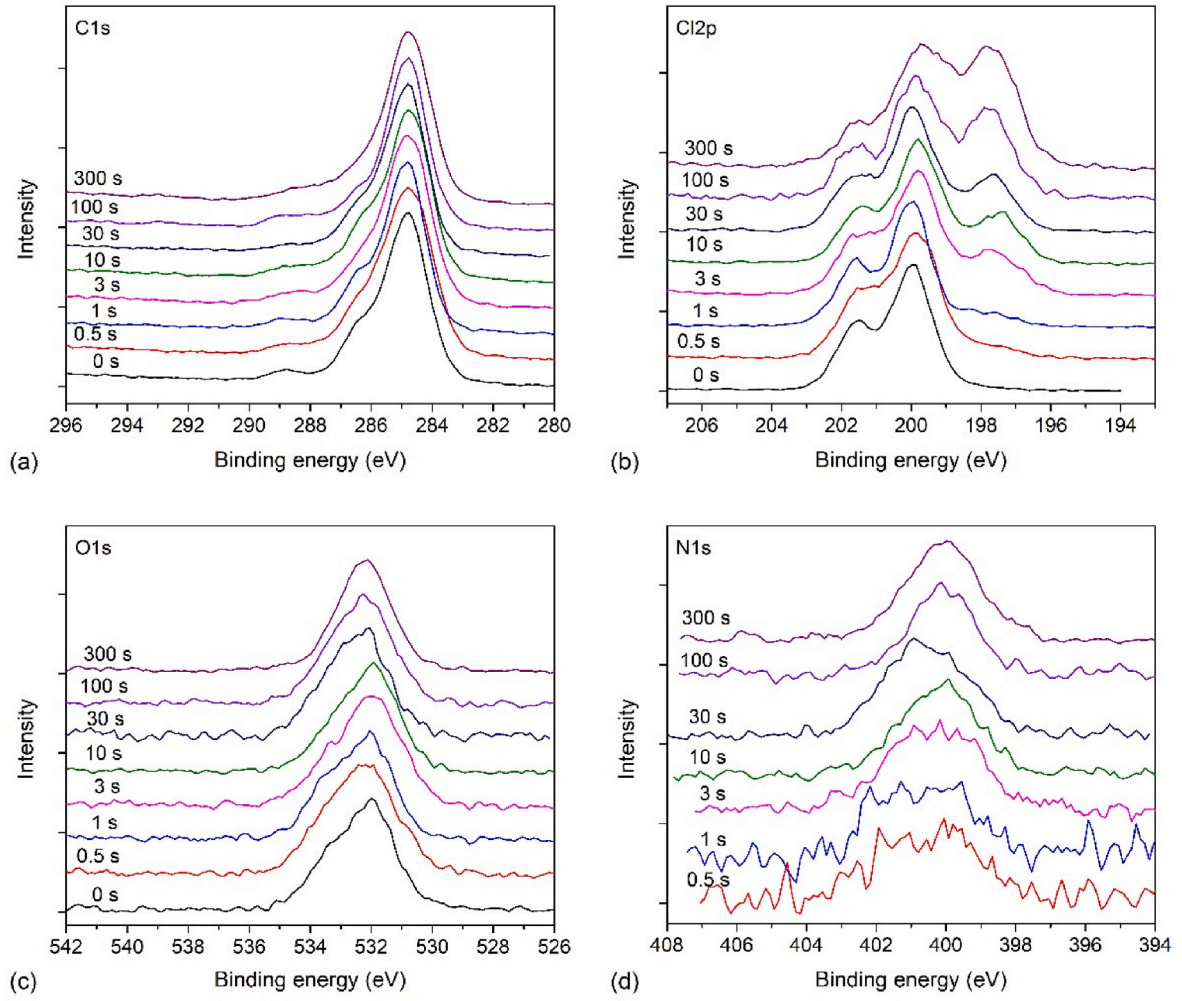

Fig. 6. High-resolution C1s spectra of carbon (a), chlorine (b), oxygen (c), and nitrogen (d) for PVC samples treated with ammonia plasma.

This doublet is characteristic of the C-Cl bond [47], and indicates the covalent bond between chlorine and carbon atoms [48], i.e., chlorination of the polymer backbone typical for pure PVC. The plasma treatment causes a gradual decrease in this doublet, and the simultaneous appearance of another peak at approximately 197.8 eV. This peak is correlated to the ionic chlorine not bonded to carbon [48]. In fact, it is a doublet, but the second $2p_{1/2}$ peak of Cl^- is at approximately 199.5 eV and partially overlaps with the $2p_{3/2}$ peak at 200 eV, as shown in Fig. 7 (a). The evolution of the high-resolution Cl2p peak therefore indicates degradation of the PVC surface film, as probed by XPS, and the formation of HCl. The proposed reaction could be either due to bond scission upon interaction of PVC with plasma radicals or charged particles, or irradiation with photons emitted from highly excited species. The latter explanation will become more feasible when discussing the modification when using a two-step plasma treatment (section 3.2.2).

An example of deconvoluting the chlorine peak is shown in Fig. 7 (a).

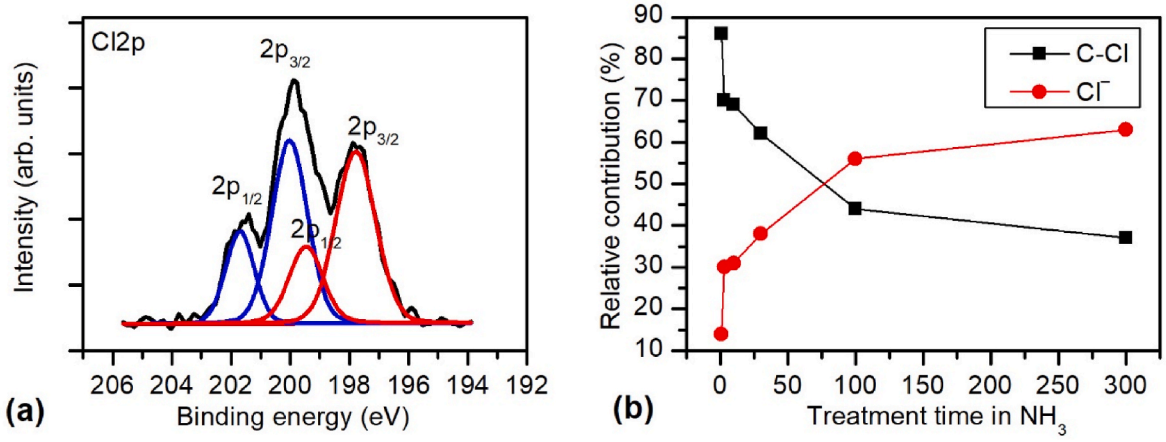

Fig. 7. An example of a composition of a chlorine peak of a sample treated for 100 s in ammonia plasma (a), and the relative proportions of different Cl states (b).

We took the peak measured after treating a PVC sample for 100 s in ammonia plasma. The subpeaks fit well with the measured curve and prove the existence of both covalently bonded and ionic chlorine. As already mentioned, the escape depth of photoelectrons is several nm, so the coexistence of the covalent and ionic chlorine may be an XPS artefact, for example, a very thin layer containing predominantly ionic chlorine on the surface of the bulk polymer containing covalently bonded chlorine. The intensity of the chlorine peak (doublet), which corresponds to ionic chlorine, increases with increasing treatment time in ammonia plasma. The spectra shown in Fig. 6(b) were fitted (as illustrated in Fig. 7(a)) to determine the ratio of the two chlorine states, and the results are summarized in Fig. 7(b).

The high-resolution oxygen peaks (Fig. 6 (c)) do not show much difference during plasma treatment. It may indicate that oxygen remains in the original chemical state (typical for plasticizers), but another explanation could be that the chemical shifts of oxygen are marginal in organic materials. The same applies to the evolution of the nitrogen peak, which is shown in Fig. 6 (d).

3.2.2. *Evolution of surface functional groups upon two-step treatment (pretreatment with hydrogen plasma followed by treatment with ammonia plasma)*

A set of PVC samples was modified using a two-step plasma treatment. In the first step, hydrogen was introduced after evacuation of the discharge tube, and hydrogen plasma was sustained for 1 s. Such plasma represents a powerful source of vacuum ultraviolet (VUV) radiation [49], and the dissociation fraction of hydrogen molecules is approximately 10 % [50]. Such a treatment causes extensive bond scission in the surface film because of the absorption of VUV radiation. The penetration depth of VUV radiation for PVC is yet to be reported, but it should be well above the escape depth of photoelectrons [51]. After treating the samples with hydrogen plasma, the reactor was evacuated to the ultimate pressure, but not vented. Instead, ammonia was introduced into the reactor, so the PVC samples, which had been pretreated with hydrogen plasma, were exposed to ammonia radicals in the second step without breaking the vacuum. The ammonia-plasma treatment parameters were the same as in subsection 3.2.1.

The XPS survey spectra for samples pretreated with hydrogen plasma are shown in Fig. 8. They are not much different from the spectra in Fig. 5, except that the chlorine peak practically vanishes after hydrogen plasma treatment and reappears only after prolonged ammonia plasma treatment. The composition, as deduced from XPS survey spectra, is shown in Table 2. The disappearance of the chlorine peak from the surface film after pretreating with hydrogen plasma is explained by the synergy between VUV radiation and H atoms during the treatment with hydrogen plasma. The VUV photons break bonds between carbon and chlorine in PVC, and the released Cl atoms react with hydrogen to form HCl molecules, which are desorbed from the polymer surface under vacuum conditions. The remaining dangling bond is occupied by an H atom. The net effect of treating PVC with hydrogen plasma is thus the depletion of chlorine. The effect has already been explained for another halogenated polymer, i.e., polytetrafluoroethylene (PTFE – Teflon) [50]. The composition and structure of PVC and PTFE differ, but the basic effect should be very similar, because the binding energy of both C-Cl and C-F bonds is well below the energy of VUV photons.

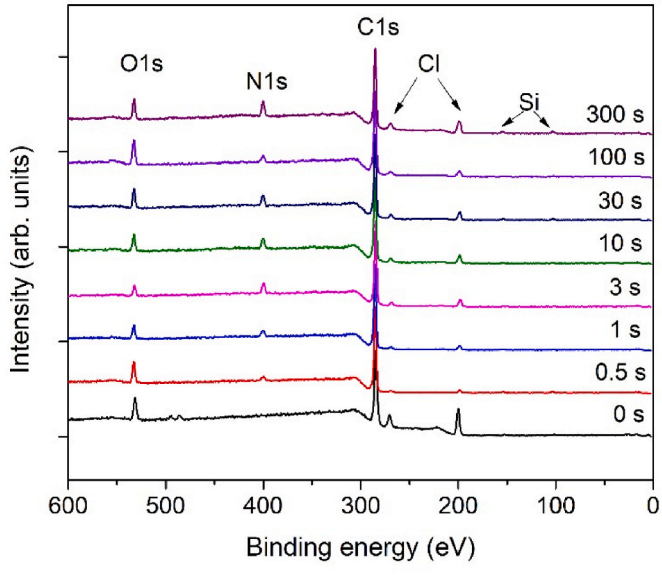

Fig. 8. The survey spectra of PVC samples pretreated with hydrogen plasma and subsequently with ammonia plasma. The treatment time in ammonia plasma is the parameter.

A similar trend is revealed for oxygen, except that it is not as pronounced as for chlorine: The oxygen concentration drops to half of the original value after pretreating with hydrogen plasma and ammonia plasma for a few seconds, and slowly recovers after prolonged treatment with ammonia plasma. Here, it is worth mentioning that the residual atmosphere in our experimental system is predominantly water vapor. The OH peak at 309 nm is even revealed in the optical spectrum shown in Fig. 2. The OH radicals represent a source of oxygen, so the concentration, as probed by XPS (Fig. 8 and Table 2), remains moderate even though the samples are exposed to VUV radiation and H atoms. Another possible explanation for a moderate concentration of oxygen in the surface film of plasma-treated samples is post-oxidation because the plasma-treated samples are exposed to air before the XPS analyses.

The slow recovery of both chlorine and oxygen on the polymer surface with increasing ammonia treatment time may be explained by the gradual etching of the surface film upon treatment with NH_x radicals. The hydrogenated carbon interacts chemically with the radicals formed in ammonia plasma, and the erosion rate is roughly 0.1 nm/s [25]. Taking into account such a low erosion rate, the ammonia plasma should not etch much of the surface film modified by a brief treatment (say up to a few s), but prolonged treatment will remove the entire modified layer and the resultant concentration of Cl and O in the surface film probed by XPS should be the same as for untreated PVC. The results shown in Fig. 8 and summarized in Table 2 confirm this model for the evolution of surface compositions of samples pretreated with hydrogen plasma.

The scission of C-Cl bonds in the polymer backbone upon irradiation with VUV photons during the hydrogen plasma pretreatment is further confirmed by high-resolution XPS spectra, which are shown in Fig. 9. Particularly relevant is the behavior of the chlorine peak, shown in Fig. 9 (b). The doublet typical for C-Cl covalent bonds practically vanishes even after the hydrogen plasma pretreatment. After pretreating with hydrogen plasma and then treating with ammonia plasma for short times (e.g., up to 30 s), the Cl2p peak is observed at values typical of Cl^- [48]. Such a huge difference in the Cl2p peak indicates that a small concentration of Cl (about 2 at.%), as observed in Fig. 8 and Table 2, should be in the ionic form, and not bonded covalently to the PVC chain.

Table 2
The composition of the surface film for samples pretreated with hydrogen plasma and subsequently treated with ammonia plasma.

Time (s)	C (at. %)	N (at. %)	O (at. %)	Si (at. %)	Cl (at. %)	O/C	N/C	Cl/C
0	78.4	0.0	10.2	1.0	10.4	0.13	0.00	0.13
0.5	85.5	5.9	5.8	0.7	2.2	0.07	0.07	0.03
1	85.5	5.9	5.8	0.7	2.2	0.07	0.07	0.03
3	82.7	8.2	5.6	0	3.6	0.07	0.10	0.04
10	80.9	7.7	7.6	0.2	3.6	0.09	0.09	0.04
30	78.7	7.6	8.4	1.7	3.5	0.11	0.10	0.04
100	79.9	7.6	6.8	1.2	4.5	0.09	0.10	0.06
300	73.3	10.0	9.0	1.8	6.0	0.12	0.14	0.08

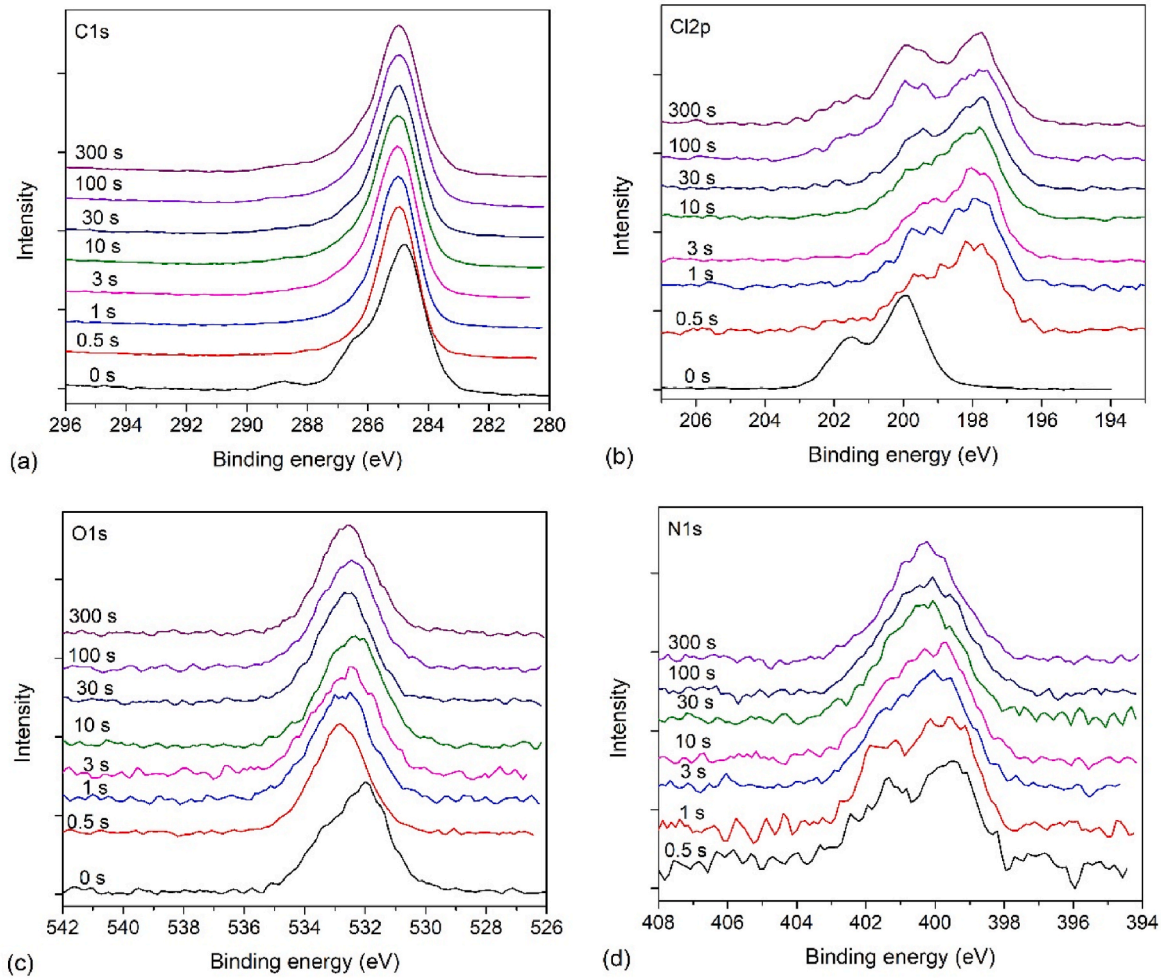

Fig. 9. High-resolution C1s spectra of carbon (a), chlorine (b), oxygen (c), and nitrogen (d) for PVC samples pretreated with hydrogen plasma and subsequently treated with ammonia plasma.

The VUV radiation thus effectively changes the structure of the PVC film at least up to the depth probed by XPS. The possible toxicity implications of VUV-induced degradation products are yet to be investigated.

The doublet typical for C-Cl covalent bonds (at 200 and 201.7 eV) slowly recovers after prolonged treatment with ammonia plasma (upper curves in Fig. 9 (b)). It is unlikely that ammonia plasma would cause the re-establishment of covalent bonds, so the possible explanation for the behavior of the Cl2p peak is gradual etching of the highly modified surface film. The chemical neighborhood of chlorine after two-step treatment for the longest treatment time (uppermost curve in Fig. 9 (b)) thus becomes similar to that treated with a single step (uppermost curve in Fig. 6 (b)). The similarity of these curves also explains why H_2 pretreatment accelerates initial N incorporation but does not affect the saturation level (Fig. 10). The brief treatment with hydrogen plasma causes destruction of the PVC surface film, which becomes prone to bonding nitrogen. That is why the N concentration reaches 6 at.% after treating H_2-pre-treated samples for only 300 ms in ammonia plasma. Moreover, ammonia plasma is sustained at a much lower discharge power, so the evolution of the nitrogen concentration is much more gradual. After prolonged treatment, however, the H_2 pretreatment becomes obsolete because the ammonia plasma itself does the job.

An interesting comparison is the nitrogen concentration of the surface film, as probed by XPS, for samples treated with ammonia plasma using a single-step (subsection 3.2.1) and a double-step (subsection 3.2.2) method. The result is shown in Fig. 10. The measured points are somehow scattered, but the trend is obvious: the nitrogen concentration

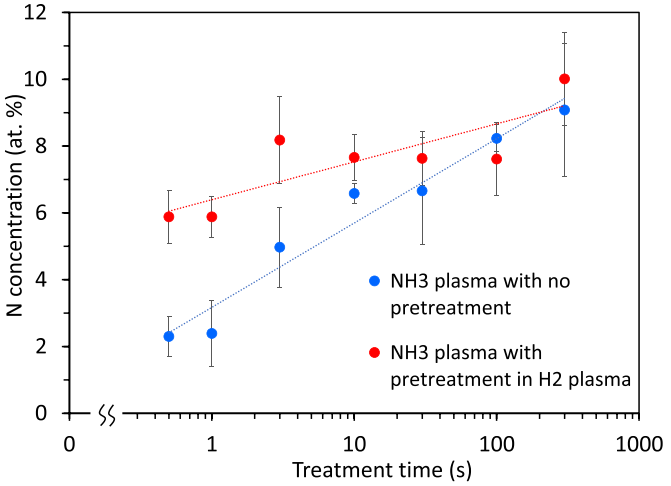

Fig. 10. The composition of the surface film as a function of treatment time in ammonia plasma. Blue – single-step treatment with ammonia plasma only; Red dots – double-step (pretreatment with hydrogen plasma followed by treatment with ammonia plasma.

increases linearly in the graphs where the x-axis is logarithmic and the y-axis is linear. This means that the nitrogen concentration increases logarithmically with increasing treatment time. Such behavior indicates

extensive functionalization of pristine PVC. Once a good surface coverage with nitrogen is achieved, the functionalization slows down. In a simple model of a perfectly smooth surface grafted with nitrogen groups, the N concentration should be stabilized. The polymers, however, are neither perfectly smooth nor is the grafting the only surface reaction. As already mentioned, the NH_x radicals not only graft to the polymer surfaces but also cause gradual etching. The etching process is supposed to be much slower than surface grafting with specific functional groups, because the grafting probability [52] is much larger than the chemical reactions that lead to etching of the same material [53].

The comparison between the two curves in Fig. 10 also reveals the beneficial effect of hydrogen plasma pretreatment. The shortest feasible treatment time with ammonia plasma (0.5 s) enables the N concentration of 2 at.% when using a single-step treatment, and as much as about 6 at.% when combining with the hydrogen plasma pretreatment. The effect is explained by the benefit of pretreatment with VUV radiation from hydrogen plasma. The radiation causes dangling bonds on the surface of the halogenated polymer, and the bonds are likely to be occupied by the plasma radicals from ammonia plasma. Similar effects were observed when treating a fluorinated polymer with hydrogen plasma, which was rich in VUV radiation [54].

The proposed VUV-induced bond-scission mechanism for Cl^- formation is consistent with the classical literature on radiation damage to polymers upon exposure to VUV lamps. F. Truica-Marasescu et al. [55] treated two types of polyolefins with VUV radiation from a commercial krypton lamp. The polymer samples were in an ammonia atmosphere, and the evolution of nitrogen concentration as probed by XPS versus irradiation time was studied. A nitrogen concentration exceeding 20 at.% was observed after prolonged treatment, and hydrophobic recovery was suppressed compared to plasma-treated samples. This was explained by subsurface crosslinking due to VUV irradiation, which should reduce molecular mobility. De Marneffe et al. [56] treated highly porous organosilicate glass dielectrics with VUV photons and reported methyl bond depletion, which was found detrimental for the dielectric properties of thin films of this material. The dehydrogenation of the methyl group was also reported by Bruce et al. [57], who treated several polymers with VUV radiation generated by argon plasma. The effects of VUV irradiation were separated by placing a MgF_2 window between the plasma and polymer samples, and the authors also found degradation of the styrene and ester groups.

Kuyyakanont and Iwata studied the degradation of several polymers, including industrial-grade PVC [58]. Polymer foils were exposed to VUV radiation arising from deuterium and xenon lamps. They found that polyvinyl chloride shows much higher sensitivity to VUV irradiation compared to near ultraviolet (NUV) irradiation and that there is a requirement for irradiation with shorter wavelengths to cause carbon-chlorine bond homolysis. Significant modifications of polymers due to treatment with VUV radiation arising from a deuterium lamp were also reported by Belmonte et al. [59].

Finally, it is worth noting that ammonia plasma should also emit VUV radiation, but it is orders of magnitude weaker than in hydrogen plasma. Fig. 2 reveals significant radiation of the hydrogen atoms in the visible range. The observed Balmer series arises from radiation from highly excited atoms to the first excited state. The radiation is much stronger in transitions to the ground state – Lyman atomic H series, but these are not detectable by the spectrometer. The discharge power selected for sustaining ammonia plasma was much lower than for hydrogen plasma (about 20 times), and the electron energy in ammonia plasma is spent on various endothermic reactions, so the VUV radiation arising from ammonia plasma should be at least 20 times less intense than for hydrogen plasma. Furthermore, excited hydrogen molecules also radiate in the VUV range (Werner and Lyman molecular bands), and the density of H_2 molecules in ammonia plasma at the same pressure as hydrogen plasma is much lower, so one can speculate that the VUV radiation from hydrogen plasma used in our experiment is at least 2 orders of magnitude larger than that from ammonia plasma.

The selected discharge parameters used in these experiments enabled gradual functionalization with nitrogen functional groups during the one-step treatment (blue line in Fig. 10) and a more rapid functionalization when using the two-step method (red line). Similar results are expected in different plasma reactors as long as the key plasma parameters (fluxes of ions, radicals, and VUV photons) are roughly the same as in our reactor. The upscaling to larger plasma systems is feasible, provided plasma is sustained in dielectric (preferably glass) tubes at a similar pressure and similar power density. It is necessary to note that the production of radicals and ions in low-pressure reactors is governed by the power density, while the loss by surface reactions. Metallic chambers should be avoided because the loss of radicals on the surface of metals is often much more intensive than on dielectrics. Furthermore, capacitive coupling in metallic chambers may cause weak sputtering of the material from the powered electrode, leading to the deposition of a minor quantity of electrode material on the polymer samples [60].

As already mentioned, plasma treatment often causes weak etching and thus morphological changes of the polymer surface on the nanometer scale. Macroscopic morphology is not affected when using such a mild plasma (the power was only 25 W when treating PVC samples with plasma sustained in ammonia) or such a short treatment time (1 s when using hydrogen plasma). The morphology on the nanometer scale was probed by AFM. Fig. 11 represents typical images. Fig. 11 (a) is an AFM image of an untreated PVC sample, and Fig. 11 (b) for the sample pretreated with hydrogen plasma and then treated with ammonia plasma for 100s. There is no significant difference between the samples, so one can conclude that the treatments do not cause morphology modification. The nanostructuring (even if it occurs) should not affect surface functionalization, but any influence of surface morphology on the biocompatibility of plasma-treated PVC within the parameter range reported in this article has yet to be determined.

4. Conclusions

Systematic treatment of medical-grade polyvinyl chloride with ammonia plasma enabled an insight into the complex mechanism of surface functionalization with nitrogen-containing functional groups. Both single-step treatment of PVC with ammonia plasma and the double-step treatment, with hydrogen plasma pretreatment, enable functionalization with nitrogen functional groups, with their concentration approaching 10 at.% after a few minutes of treatment with ammonia plasma. Both treatments, however, also cause the degradation of the covalent C-Cl bond and the formation of ionic chlorine bonds. The latter should be in the form of HCl, whose concentration is easily detectable by XPS because of the significant peak shift. Mild treatment with ammonia plasma only (say up to a few seconds) enables functionalization with approximately 4 at.% nitrogen without significant damage to the covalent C-Cl bond. Even 1 s of hydrogen plasma pretreatment, however, destroys this bond in the surface film of the thickness corresponding to the escape depth of photoelectrons, so the double-step method may not be applicable to medical practice. Any influence of the shift from covalent to ionic chlorine states on the biocompatibility, and thus the suitability for medical use, of plasma-treated PVC is yet to be studied.

CRediT authorship contribution statement

Rok Zaplotnik: Writing – review & editing, Visualization, Investigation, Data curation. **Nina Recek:** Methodology, Investigation, Formal analysis. **Gregor Primc:** Validation, Supervision, Resources, Project administration. **Andrej Gyergyek:** Validation, Supervision, Conceptualization. **Marian Lehocky:** Validation, Supervision, Funding acquisition. **Miran Mozetič:** Writing – review & editing, Writing – original draft, Resources, Funding acquisition. **Alenka Vesel:** Writing – review & editing, Visualization, Investigation, Formal analysis, Data curation.

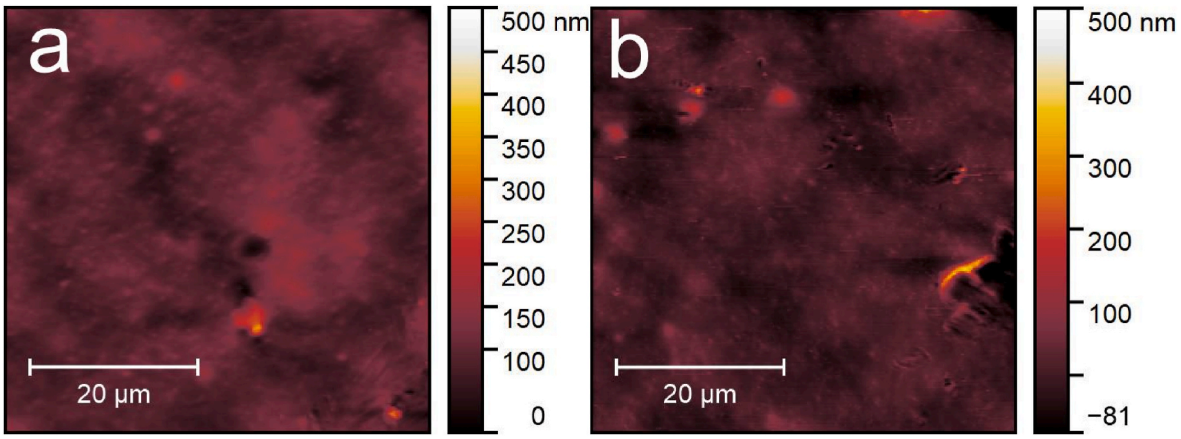

Fig. 11. AFM images of an untreated PVC sample (a) and the sample pretreated with hydrogen plasma for 1 s and subsequent treatment in ammonia plasma for 100 s (b). The arithmetical mean roughness (S_a) as deduced from the images was 23 and 21 nm, respectively.

Declaration of competing interest

The authors declare that they have no known competing financial interests or personal relationships that could have appeared to influence the work reported in this paper.

Acknowledgements

This research was funded by the Slovenian Research Agency, project L7-60162 “Application of VUV radiation and plasma radicals for adequate wettability of plastic housings” and core funding P2-0082 “Thin-film structures and plasma surface engineering”. M. L. gratefully acknowledges the support from the Ministry of Education, Youth and Sports of the Czech Republic (grant RP/CPS/2024-28/005).

Data availability

Data will be made available on request.

References

[1] Dors, M., 2021. Plasma: from materials to emerging technologies. Appl. Sci. 11, 8311. https://doi.org/10.3390/app11188311.
[2] Zhang, Z., Hu, C., Qin, Q.-H., 2025. The improvement of void and interface characteristics in fused filament fabrication-based polymers and continuous carbon fiber-reinforced polymer composites: a comprehensive review. Int. J. Adv. Manuf. Technol. 137, 1047. https://doi.org/10.1007/s00170-025-15240-4.
[3] Barjasteh, A., Kaushik, N., Choi, E.H., Kaushik, N.K., 2024. Cold atmospheric pressure plasma solutions for sustainable food packaging. Int. J. Mol. Sci. 25, 6638. https://doi.org/10.3390/ijms25126638.
[4] Primc, G., Mozetič, M., 2024. Surface modification of polymers by plasma treatment for appropriate adhesion of coatings. Materials 17, 1494. https://doi.org/10.3390/ma17071494.
[5] Zhang, J., Lv, S., Zhao, X., Ma, S., Zhou, F., 2024. Surface functionalization of polyurethanes: a critical review. Adv. Colloid Interface Sci. 325, 103100. https://doi.org/10.1016/j.cis.2024.103100.
[6] Karthik, C., Mavelil-Sam, R., Thomas, S., Thomas, V., 2024. Cold plasma technology based eco-friendly food packaging biomaterials. Polymers 16, 230. https://doi.org/10.3390/polym16020230.
[7] Dufour, T., 2023. From basics to frontiers: a comprehensive review of plasma-modified and plasma-synthesized polymer films. Polymers 15, 3607. https://doi.org/10.3390/polym15173607.
[8] Li, R., Li, Y., Bai, Y., Yi, P., Sun, C., Shi, S., Gong, Y.K., 2024. Achieving superior anticoagulation of endothelial membrane mimetic coating by heparin grafting at zwitterionic biocompatible interfaces. Int. J. Biol. Macromol. 257, 128574. https://doi.org/10.1016/j.ijbiomac.2023.128574.
[9] Hsu, C.-N., Lin, C.-C., Lin, Y.-T., Chen, Y.-H., Chou, P.-H., Chang, Y.-J., Tseng, T.-Y., Lin, Z.-Y., Hong, S.-G., Cheng, M.-T., Chen, Y., Yao, C.-L., 2024. Surface modification of aligned electrospun poly(3-hydroxybutyrate-co-3-hydroxyvalerate)-based scaffold for binding with fibronectin or collagen in vascular tissue engineering. J. Taiwan Inst. Chem. Eng. 160, 105279. https://doi.org/10.1016/j.jtice.2023.105279.
[10] Chang, J., Yu, L., Lei, J., Liu, X., Li, C., Zheng, Y., Chen, H., 2023. A multifunctional bio-patch crosslinked with glutaraldehyde for enhanced mechanical performance, anticoagulation properties, and anti-calcification properties. J. Mater. Chem. B 11, 10455. https://doi.org/10.1039/D3TB01724A.
[11] Shi, S., Wei, X., Peng, X., Pu, X., Feng, S., Gao, X., Yu, X., 2025. An oxidized chondroitin sulfate-crosslinked and CuCDs-loaded decellularized bovine pericardium with improved anticoagulation, pro-endothelialization and anti-calcification properties for BHVs. J. Mater. Chem. B 13, 7196. https://doi.org/10.1039/D5TB00827A.
[12] Li, L., An, D., Zhao, J., Yu, Y., Zeng, Y., Yang, X., Yu, Q., Kang, K., Wu, Y., Yi, Q., 2025. Versatile coating via programmed assembly of miR-155 inhibitor and endothelial affinity peptide. J. Biomed. Mater. Res., Part A 113, e37923. https://doi.org/10.1002/jbm.a.37923.
[13] Yang, J., Gu, Y., Wang, T., Zhang, J., Zhang, X., Yu, F., 2025. The multifaceted roles of thrombomodulin: anticoagulation, anti-inflammation, and anti-tumor potential. Curr. Pharm. Des. 31, 1673. https://doi.org/10.2174/0113816128335289241218161938.
[14] Zhu, Q., Ye, P., Guo, F., Zhu, Y., Nan, W., Chang, Z., 2022. A heparin-functionalized covered stent prepared by plasma technology. J. Biomater. Appl. 36, 1243. https://doi.org/10.1177/08853282211051871.
[15] Garg, H.G., Linhardt, R.J., Hales, C.A., 2005. Chemistry and Biology of Heparin and Heparan Sulfate. Elsevier Science, Amsterdam.
[16] Liao, D., Wang, X., Lin, P.H., Yao, Q., Chen, C., 2009. Covalent linkage of heparin provides a stable anticoagulation surface of decellularized porcine arteries. J. Cell Mol. Med. 13, 2736. https://doi.org/10.1111/j.1582-4934.2008.00589.x.
[17] Fan, Y., Zhu, T., Li, Z., Li, J., Ren, F., Gao, Z., Li, A., Zhu, L., Huang, Z., 2025. Non-equilibrium plasma cracking assisted ammonia marine engine for zero carbon emissions. Int. J. Hydrogen Energy 112, 433. https://doi.org/10.1016/j.ijhydene.2025.02.341.
[18] He, Y., Zhu, N., Cai, Y., 2025. Research on hydrogen production from ammonia decomposition by pulsed plasma catalysis. Molecules 30, 1054. https://doi.org/10.3390/molecules30051054.
[19] Bayer, B.N., Bhan, A., Bruggeman, P.J., 2024. Reaction pathways and energy consumption in NH3 decomposition for H2 production by low temperature, atmospheric pressure plasma. Plasma Chem. Plasma Process. 44, 2101. https://doi.org/10.1007/s11090-024-10501-8.
[20] Van Steenweghen, F., Verschueren, A., Fedirchyk, I., Martens, J.A., Bogaerts, A., Hollevoet, L., 2025. Reversed plasma catalysis process design for efficient ammonia decomposition. ACS Sustain. Chem. Eng. 13, 737. https://doi.org/10.1021/acssuschemeng.4c08899.
[21] Niu, Y.-L., Li, S.-Z., Wang, X.-C., Yu, Q.-K., Yang, D., Wen, X., Zhang, J., 2024. Characteristic study of nitrogen microwave plasma decomposition of ammonia at atmospheric pressure for hydrogen production. Plasma Sources Sci. Technol. 33, 105018. https://doi.org/10.1088/1361-6595/ad7ea4.
[22] Cheng, G., Liu, X., Xiong, J., 2024. Recent advances in coupling pollutants degradation with hydrogen production by semiconductor photocatalysis. Chem. Eng. J. 501, 157491. https://doi.org/10.1016/j.cej.2024.157491.
[23] Draškovič-Bračun, A., Mozetič, M., Zaplotnik, R., 2018. E- and H-mode transition in a low pressure inductively coupled ammonia plasma. Plasma Process. Polym. 15, 1700105. https://doi.org/10.1002/ppap.201700105.
[24] Vesel, A., Zaplotnik, R., Primc, G., Liu, X., Xu, K., Chen, K.C., Wei, C., Mozetic, M., 2016. Functionalization of polyurethane/urea copolymers with amide groups by polymer treatment with ammonia plasma. Plasma Chem. Plasma Process. 36, 835. https://doi.org/10.1007/s11090-016-9696-3.
[25] Drenik, A., Mourkas, A., Zaplotnik, R., Primc, G., Mozetič, M., Panjan, P., Alegre, D., Tabarés, F.L., 2016. Erosion of a-C:H in the afterglow of ammonia plasma. J. Nucl. Mater. 475, 237. https://doi.org/10.1016/j.jnucmat.2016.04.011.
[26] Young, E.R., Martin, C., Ribaudo, J., Xia, X., Moritz, W.R., Madira, S., Zayed, M.A., Sacks, J.M., Li, X., 2024. Surface modification of PEEKs with cyclic peptides to support endothelialization and antithrombogenicity. Mater. Today Commun. 39, 108664. https://doi.org/10.1016/j.mtcomm.2024.108664.
[27] Islam, M., Matouk, Z., Ouldhamadouche, N., Pireaux, J.-J., Achour, A., 2023. Plasma treatment of polystyrene films—Effect on wettability and surface

interactions with Au nanoparticles. Plasma 6, 322. https://doi.org/10.3390/plasma6020022.
[28] Buddhadasa, M., Verougstraete, B., Gomez-Rueda, Y., Petitjean, D., Denayer, J.F. M., Reniers, F., 2023. A study of plasma–porous carbon–CO_2 interactions: ammonia plasma treatment and CO_2 capture. J. CO2 Util. 68, 102388. https://doi.org/10.1016/j.jcou.2022.102388.
[29] Peixoto, T., Silva, D., Rodrigues, M., Neto, M., Silva, R., Paiva, M.C., Grenho, L., Fernandes, M.H., Lopes, M.A., 2023. Amination of polymeric braid structures to improve tendon healing: an experimental comparison. Macromol. Mater. Eng. 308, 2200426. https://doi.org/10.1002/mame.202200426.
[30] Mora-Cortes, L.F., Rivas-Muñoz, A.N., Neira-Velázquez, M.G., Contreras-Esquivel, J.C., Roger, P., Mora-Cura, Y.N., Soria-Arguello, G., Bolaina-Lorenzo, E. D., Reyna-Martínez, R., Zugasti-Cruz, A., Narro-Céspedes, R.I., 2022. Biocompatible enhancement of poly(ethylene terephthalate) (PET) waste films by cold plasma aminolysis. J. Chem. Technol. Biotechnol. 97, 3001. https://doi.org/10.1002/jctb.7106.
[31] Benlikaya, R., Slobodian, P., Riha, P., Puliyalil, H., Cvelbar, U., Olejnik, R., 2022. Ammonia plasma-treated carbon nanotube/epoxy composites and their use in sensing applications. Express Polym. Lett. 16, 85. https://doi.org/10.3144/expresspolymlett.2022.7.
[32] Vesel, A., Zaplotnik, R., Primc, G., Mozetič, M., Katan, T., Kargl, R., Mohan, T., Kleinschek, K.S., 2021. Rapid functionalization of polytetrafluorethylene (PTFE) surfaces with nitrogen functional groups. Polymers 13, 4301. https://doi.org/10.3390/polym13244301.
[33] Deleanu, I.M., Grosu, E., Ficai, A., Ditu, L.M., Motelica, L., Oprea, O.-C., Gradisteanu Pircalabioru, G., Sonmez, M., Busuioc, C., Ciocoiu, R., Antoniac, V.I., 2024. New antimicrobial materials based on plasticized polyvinyl chloride for urinary catheters: preparation and testing. Polymers 16, 3028. https://doi.org/10.3390/polym16213028.
[34] Sheng, K., Zheng, X., Gao, Y., Long, J., Bao, T., Wang, S., 2024. Fabrication of metal-organic frameworks containing Cu^{2+} coated medical PVC catheters with durable antiplatelet and antibacterial activities. Colloids Surf. A Physicochem. Eng. Asp. 700, 134779. https://doi.org/10.1016/j.colsurfa.2024.134779.
[35] Ali, S., Khan, O.S., Youssef, A.M., Saba, I., Alfedaih, D., 2024. Hydrophilic catheters for intermittent catheterization and occurrence of urinary tract infections. A retrospective comparative study in patients with spinal cord injury. BMC Urol. 24, 122. https://doi.org/10.1186/s12894-024-01510-y.
[36] Tarabal, V.S., Abud, Y.K.D., da Silva, F.G., da Cruz, L.F., Fontes, G.N., da Silva, J. A., Filho, C.B.S., Sinisterra, R.D., Granjeiro, J.M., Granjeiro, P.A., 2023. Effect of DMPEI coating against biofilm formation on PVC catheter surface. World J. Microbiol. Biotechnol. 40, 6. https://doi.org/10.1007/s11274-023-03799-7.
[37] Zhang, Y., Man, J., Wang, J., Liu, J., Song, X., Yu, X., Li, J., Li, R., Qiu, Y., Li, J., Chen, Y., 2024. Surface modification of polyvinyl chloride with sodium alginate/carboxymethyl chitosan and heparin for realizing the anticoagulation. Int. J. Biol. Macromol. 254, 127653. https://doi.org/10.1016/j.ijbiomac.2023.127653.
[38] DEHP-free Medical Grade PVC Compounds, 2019. Changyoung Chemical Co., Ltd. (Accessed 12 May 2025)
[39] Campisi, L., La Motta, C., Napierska, D., 2025. Polyvinyl chloride (PVC), its additives, microplastic and human health: unresolved and emerging issues. Sci. Total Environ. 960, 178276. https://doi.org/10.1016/j.scitotenv.2024.178276.
[40] Gilbert, M., Patrick, S., 2017. Chapter 13 - poly(vinyl chloride). In: Gilbert, M. (Ed.), Brydson's Plastics Materials, eighth ed. Butterworth-Heinemann, p. 329. https://doi.org/10.1016/B978-0-323-35824-8.00013-X.
[41] Wypych, G., 2015. 11 - principles of stabilization. In: Wypych, G. (Ed.), PVC Degradation and Stabilization, third ed. ChemTec Publishing, Boston, p. 287. https://doi.org/10.1016/B978-1-895198-85-0.50013-3.
[42] Lloyd, A., 2004. Alternatives to PVC: medical materials. Mater. Today 7, 19. https://doi.org/10.1016/S1369-7021(04)00071-9.
[43] Medical Devices Containing DEHP Plasticised PVC, 2002. Neonates and Other Groups Possibly at Risk from DEHP Toxicity. European Commission. (Accessed 5 September 2025).
[44] E. Commission, D.-G.f. Environment, Ramboll, 2022. The Use of PVC (Poly Vinyl Chloride) in the Context of a Non-toxic Environment – Final Report. Publications Office of the European Union.
[45] Kudzin, M.H., Piwowarska, D., Festinger, N., Chruściel, J.J., 2024. Risks associated with the presence of polyvinyl chloride in the environment and methods for its disposal and utilization. Materials 17, 173.
[46] Beamson, G., Briggs, D., 1992. High Resolution XPS of Organic Polymers: the Scienta ESCA300 Database. Wiley, Chichester.
[47] Wang, C., Johnson, D., Suleman, M.A., Suleman, M.A., Zhang, W., Pestov, D., Ramsinghani, P., Wickham, R., Wynne, K.J., 2015. Diffusion of di(2-ethylhexyl) phthalate in PVC quantified by ATR-IR spectroscopy. Polymer 76, 70. https://doi.org/10.1016/j.polymer.2015.08.048.
[48] Heydari Gharahcheshmeh, M., Chowdhury, K., 2024. Enhancing capacitance of carbon cloth electrodes via highly conformal PEDOT coating fabricated by the OCVD method utilizing $SbCl_5$ oxidant. Adv. Mater. Interfac. 11, 2400118. https://doi.org/10.1002/admi.202400118.
[49] Fantz, U., Briefi, S., Rauner, D., Wünderlich, D., 2016. Quantification of the VUV radiation in low pressure hydrogen and nitrogen plasmas. Plasma Sources Sci. Technol. 25, 045006. https://doi.org/10.1088/0963-0252/25/4/045006.
[50] Lojen, D., Zaplotnik, R., Primc, G., Mozetič, M., Vesel, A., 2020. Effect of VUV radiation and reactive hydrogen atoms on depletion of fluorine from polytetrafluoroethylene surface. Appl. Surf. Sci. 533, 147356. https://doi.org/10.1016/j.apsusc.2020.147356.
[51] Fouchier, M., Pargon, E., Azarnouche, L., Menguelti, K., Joubert, O., Cardolaccia, T., Bae, Y.C., 2011. Vacuum ultra violet absorption spectroscopy of 193 nm photoresists. Appl. Phys. A 105, 399. https://doi.org/10.1007/s00339-011-6553-3be.
[52] Vesel, A., Zaplotnik, R., Mozetič, M., Primc, G., 2021. Surface modification of PS polymer by oxygen-atom treatment from remote plasma: initial kinetics of functional groups formation. Appl. Surf. Sci. 561, 150058. https://doi.org/10.1016/j.apsusc.2021.150058.
[53] Doliška, A., Vesel, A., Kolar, M., Stana-Kleinschek, K., Mozetič, M., 2012. Interaction between model poly(ethylene terephthalate) thin films and weakly ionised oxygen plasma. Surf. Interface Anal. 44, 56. https://doi.org/10.1002/sia.3769.
[54] Lojen, D., Zaplotnik, R., Primc, G., Mozetič, M., Vesel, A., 2022. Optimization of surface wettability of polytetrafluoroethylene (PTFE) by precise dosing of oxygen atoms. Appl. Surf. Sci. 598, 153817. https://doi.org/10.1016/j.apsusc.2022.153817.
[55] Truica-Marasescu, F., Guimond, S., Wertheimer, M.R., 2003. VUV-induced nitriding of polymer surfaces: Comparison with plasma treatments in nitrogen. Nucl. Instrum. Methods Phys. Res. Sect. B Beam Interact. Mater. Atoms 208, 294. https://doi.org/10.1016/S0168-583X(03)00658-X.
[56] de Marneffe, J.-F., Zhang, L., Heyne, M., Lukaszewicz, M., Porter, S.B., Vajda, F., Rutigliani, V., el Otell, Z., Krishtab, M., Goodyear, A., Cooke, M., Verdonck, P., Baklanov, M.R., 2015. Vacuum ultra-violet damage and damage mitigation for plasma processing of highly porous organosilicate glass dielectrics. J. Appl. Phys. 118. https://doi.org/10.1063/1.4932202.
[57] Bruce, R.L., Engelmann, S., Lin, T., Kwon, T., Phaneuf, R.J., Oehrlein, G.S., Long, B. K., Willson, C.G., Végh, J.J., Nest, D., Graves, D.B., Alizadeh, A., 2009. Study of ion and vacuum ultraviolet-induced effects on styrene- and ester-based polymers exposed to argon plasma. J. Vac. Sci. Technol. B: Microelectron. Nanometer Struct. Process., Meas., Phenom. 27, 1142. https://doi.org/10.1116/1.3136864.
[58] Kuyyakanont, A., Iwata, M., 2024. Study of different degradation effects in UV-sensitive polymers using xenon lamp and deuterium lamp to simulate UV irradiation in space environment. Nucl. Instrum. Methods Phys. Res. Sect. B Beam Interact. Mater. Atoms 549, 165267. https://doi.org/10.1016/j.nimb.2024.165267.
[59] Belmonte, G.K., Charles, G., Strumia, M.C., Weibel, D.E., 2016. Permanent hydrophilic modification of polypropylene and poly(vinyl alcohol) films by vacuum ultraviolet radiation. Appl. Surf. Sci. 382, 93. https://doi.org/10.1016/j.apsusc.2016.04.091.
[60] Mozetič, M., 2025. Low-pressure non-equilibrium plasma technologies: scientific background and technological challenges. Rev. Modern Plasma Phys. 9, 25. https://doi.org/10.1007/s41614-025-00201-x.